The Power Grid Transient Simulation in Linear Time Based on 3D Alternating-Direction-Implicit Method

Yu-Min Lee and Charlie Chung-Ping Chen
Department of Electrical and Computer Engineering
University of Wisconsin at Madison
Madison, WI 53706
yu-min@cae.wisc.edu and chen@engr.wisc.edu

Abstract

The rising power consumption and clock frequency of VLSI technology demand robust and stable power delivery. Extensive transient simulations on large scale power delivery structures are required to analyze power delivery fluctuation caused by dynamic IR-, and Ldi/dt drop as well as package and on-chip resonance. This paper develops a novel and efficient transient simulation algorithm for the power distribution networks. The 3D TLM-ADI (Transmission-Line-Modeling Alternating-Direction-Implicit) method, first models the power delivery structure as three dimensional transmission line shunt node structure and transfers those equations to the Telegraph equation. Finally, we solve it by the alternating direction implicit method. The 3D TLM-ADI method, with linear runtime and memory requirement, is also unconditionally stable which ensures that the time-steps are not limited by any stability requirement. Numerical experimental results show that the 3D TLM-ADI method is not only over 300,000 times faster than SPICE but also extremely memory saving and accurate.

I INTRODUCTION

Due to the ever-increasing clock frequency and the aggressively shrinking feature sizes of the VLSI technology, robust power distribution network is crucial to ensure the quality of power delivery of VLSI chips. This makes the issues of the design and verification of the power grid analysis more important. The improper design of power grids can degrade the circuit performance, and the reliability. To obtain a robust design, numerous researchers studied the impact and proposed solutions of this problem [5, 3, 7, 9].

There are many sources of power fluctuation such as IR drop, Ldi/dt drop, and resonance issues. Although the IR drop can be simply examined by the DC analysis, the Ldi/dt drop issues need to be analyzed by the transient simulation due to the differentiation nature of Ldi/dt drop. Hence, extensive transient simulations are required during the design process to ensure the design quality of power delivery. [16] decoupled the power delivery structure, and transistors simulation to enhance the simulation speed. However, owing to the tremendous amount of the power delivery elements, general purpose circuit simulators such as SPICE [12] require long runtime and huge memory consumption.

Several techniques [8, 1, 10] have been developed to speed up the analysis. [8] presented the transmission matrix method to reduce the memory usage and CPU time for analysis. The method is based on a multi-input, multi-output transfer function which enables the entire power distribution network to be computed as the product of several small individual sparse square matrices. [1] developed an efficient modified nodal analysis (MNA) solver to speed up the DC and transient simulation of the power delivery circuits. This MNA Solver is based on the preconditioned Krylov-subspace iterative method which has been shown to be significantly faster than traditional iterative methods without preconditioning. Recently, EE Times reported one of the most promising method, TLM-ADI method, which was proposed by Lee and Chen [10]. They proposed to use the TLM (Transmission Line Modeling) [2] method to perform the time domain simulation. TLM is close related to the FDTD (Finite Difference Time Domain) method, which is one of the most popular and powerful computational electromagnetic techniques in the microwave simulation field [14, 15]. The TLM method differs from FDTD in the sense that it utilizes transmission line cells to model the structure and directly solves the voltage and current quantities while FDTD uses Yee cell structure to obtain electric and magnetic fields. Since voltages and currents are the major focus of the VLSI power delivery analysis, TLM method can be applied directly to perform power delivery transient simulation. The TLM method has been successfully applied to analyze the two-dimensional LC networks by Gwarek [6]. Unfortunately, the time step size is restricted by the minimum grid cell size (Courant stability condition as the standard FDTD

method [14, 15]).

Lee and Chen [10] directly solved the KCL and KVL equations by utilizing the transmission line equations. Although their method is an unconditionally stable ADI [13] (alternating-direction-implicit) scheme for the two dimensional power grid networks, it cannot be directly extended to the three dimensional power grids. In this paper, instead of solving the KCL and KVL equations, we first set up the transmission line equations of the three dimensional power grid networks. Then, we transfer those equations to the telegraph equation, and develop an unconditionally stable ADI algorithm which relaxes the time-step constraint. With this new method, the upper bound of the time step is only limited by the accuracy requirement rather than the stability requirement. Thus, it greatly lightens the computational load due to the reduction of number of time steps. Furthermore, the runtime and memory is linear with the number of total nodes N since the method only solves around $N^{2/3}$ $tridiagonal$ matrix equations with dimension $N^{1/3} \times N^{1/3}$ at each time step. Extensive experimental results show that our algorithm is not only orders of magnitude faster than SPICE but also extremely memory saving and accurate.

The remainder of the paper is organized as follows. First, the review of the finite-difference algorithm, and the relation between the modified nodal analysis (MNA), transmission-line-equations (TLE), and the telegraph equation will be studied in Section II. Then, the derivation of the 3D TLM-ADI algorithm with its two main features, unconditional stability and linear run time will be presented in Section III. Finally, the numerical experiments and conclusion of this paper will be given in Section IV, and V.

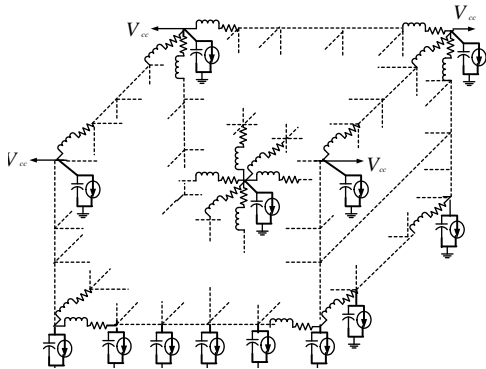## II POWER GRID MODELING AND SIMULATION WITH THE FINITE DIFFERENCE METHOD

Figure 1. Power Grids Modeling

The power distribution networks are modeled by a three dimensional shunt node structure of the transmission line grids as illustrated in Figure 1. Since the structures of the ground, and power networks are the same, Figure 1 only shows the

power delivery networks. This model results in identical formulations for both the analysis of the power and ground networks. For simplicity, in the remainder of this paper the analysis of the power distribution network is assumed. For each cell as shown in Fig 2, the wire segments are represented by resistors and inductors connected in series in $x-$ and $y-$ directions with a capacitor connected to the ground networks, and the vias are modeled as resistors and inductors connected in series in $z-$ direction. The parameters r, l, and c are resistance per unit length, inductance per unit length, and capacitance per unit length, respectively. Once the circuit model has been set up, the system matrices are created by using the transient nodal analysis. First, the KCL at the center node $O_{i,j,k}$, and
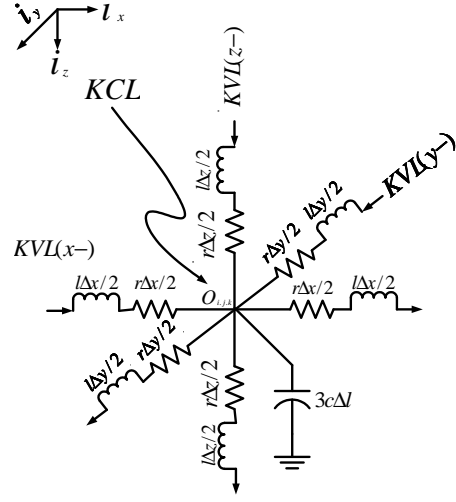

Figure 2. KCL and KVL for a cell

the KVL along the $x-$, $y-$, and $z-$ directions of the center node are applied to each cell, as shown in Figure 2. The KCL and KVL equations for a node $O_{i,j,k}$ at position (x_i, y_j, z_k) can be written as (The independent current sources have been ignored for simplicity.)

$$\tilde{\mathbf{C}}_{ijk}\frac{\partial}{\partial t}\mathbf{x}_{ijk} = -\tilde{\mathbf{G}}_{ijk}\mathbf{x}_{ijk} \qquad (1)$$

Then assembling the KVL and KCL equations for each cell, the full system equations can be represented as

$$\tilde{\mathbf{C}}\frac{\partial}{\partial t}\mathbf{x} + \tilde{\mathbf{G}}\mathbf{x} = 0 \qquad (2)$$

where $\mathbf{x}$ is the vector of nodal voltages and branch currents. The above system equations are equivalent to the modified nodal analysis (MNA) equations.

Connection Between MNA and Transmission-Line-Equations

After multiplying both sides of the Equation (1) by the inverse of $\tilde{\mathbf{C}}_{ijk}$, and approaching $\triangle x$, $\triangle y$, $\triangle z$, and $\triangle l$ to zeros with the uniform internodal distance assumption ($\triangle x =$

$\triangle y = \triangle z = \triangle l$), leads to the following equations

$$\frac{\partial v}{\partial t} = \frac{1}{3c}(-\frac{\partial i_x}{\partial x} - \frac{\partial i_y}{\partial y} - \frac{\partial i_z}{\partial z}) \quad (3)$$

$$\frac{\partial i_x}{\partial t} = \frac{1}{l}(-\frac{\partial v}{\partial x} - ri_x) \quad (4)$$

$$\frac{\partial i_y}{\partial t} = \frac{1}{l}(-\frac{\partial v}{\partial y} - ri_y) \quad (5)$$

$$\frac{\partial i_z}{\partial t} = \frac{1}{l}(-\frac{\partial v}{\partial z} - ri_z). \quad (6)$$

The above equations are the general transmission line equations which can be solved by the related techniques such as TLM and FDTD methods [14]. The procedures and concepts of the general finite difference methods for solving the three-dimensional TLE are quite simple. First, the domain ($x - y - z - t$ planes) of the solution is discretized by a net with a finite number of mesh points $(x_i, y_j, z_k, t_n) = (i\triangle x, j\triangle y, k\triangle z, n\triangle t)$ which is denoted as "$\bullet_{i,j,k}^n$". After the discretization, the derivatives at each mesh point are replaced by the finite difference such as forward-, backward-, or central- difference.

Applying the central difference method into Equations (3)–(6), we can get a simple explicit finite difference updating scheme which is an extension of the two dimensional circuit [6]. Each nodal voltage and branch current at each time step can be easily solved since only one unknown variable appears in each difference equation. While this scheme suffers on the Courant stability constraint [14, 15] which is

$$\triangle t \le \frac{1}{\frac{1}{\sqrt{lc}}\sqrt{\frac{1}{(\triangle x)^2} + \frac{1}{(\triangle y)^2} + \frac{1}{(\triangle z)^2}}}. \quad (7)$$

As the feature size of VLSI technology decreasing to 0.1 μm, and $1/\sqrt{lc}$ being a half of the light speed, the Courant limit is close to 0.3838 fs. Thus it needs around 2.57×10^6 time steps to simulate a 1-ns period.

Connection Between TLE and Telegraph-Equation

In order to solve Equations (3)–(6), we can first differentiate Equations (3)–(6) with respect to t, x, y, and z, then combine the results with Equation (3). This leads to a telegraph equation as

$$\frac{\partial^2 v}{\partial t^2} + a\frac{\partial v}{\partial t} - b(\frac{\partial^2 v}{\partial x^2} + \frac{\partial^2 v}{\partial y^2} + \frac{\partial^2 v}{\partial z^2}) = 0 \quad (8)$$

where $a = r/l$, and $b = 1/3lc$.

Hence, we can solve the telegraph equation (8) instead of solving the transmission line equations (3)–(6). Extending the one dimensional simple implicit FDTD method [11] of the telegraph equation to the above three dimensional telegraph equa-

tion, Equation (8) becomes to

$$\frac{v_{i,j,k}^{n+1} - 2v_{i,j,k}^n + v_{i,j,k}^{n-1}}{(\triangle t)^2} + a\frac{v_{i,j,k}^{n+1} - v_{i,j,k}^{n-1}}{2\triangle t}$$
$$-b\left\{\frac{v_{i+1,j,k}^{n+1} - 2v_{i,j,k}^{n+1} + v_{i-1,j,k}^{n+1}}{(\triangle x)^2} + \frac{v_{i,j+1,k}^{n+1} - 2v_{i,j,k}^{n+1} + v_{i,j-1,k}^{n+1}}{(\triangle y)^2}\right.$$
$$\left. + \frac{v_{i,j,k+1}^{n+1} - 2v_{i,j,k}^{n+1} + v_{i,j,k-1}^{n+1}}{(\triangle z)^2}\right\} = 0 \quad (9)$$

Although this simple implicit scheme is unconditionally stable, we need to solve a heptadiagonal system of algebraic equations at each time step. Therefore, the computational time is extremely huge.

III THE 3D TLM-ADI METHOD

In this section, we will derive the 3D TLM-ADI scheme of the simple implicit FDTD method (9) by using an general ADI procedure [4]. After the derivation, the two main features of the 3D TLM-ADI algorithm, unconditional stability and linear run time, will be dressed. Finally, we will extend our proposed method to the power grids with nonuniform internodal distances.

The ADI method is a well known method for solving the partial differential equation (PDE). The main feature of ADI is to sweep directions alternately. In contrast to the standard finite difference formulation with only one iteration to advance from the nth to $(n+1)^{th}$ time step, the formulation of ADI method requires multi-level intermediate steps to advance from the nth to $(n+1)^{th}$ time step.

The Equation (9) can be rewritten as

$$(I + \sum_{m=1}^{3} A_m)v_{i,j,k}^{n+1} - 2c_0v_{i,j,k}^n + c_1v_{i,j,k}^{n-1} = 0 \quad (10)$$

where the operators of I, A_m's, and the constants of c_0, c_1 are defined as

$$Iv_{i,j,k}^n \triangleq v_{i,j,k}^n \quad (11)$$

$$A_1v_{i,j,k}^n \triangleq -\rho_x(v_{i+1,j,k}^n - 2v_{i,j,k}^n + v_{i-1,j,k}^n) \quad (12)$$

$$A_2v_{i,j,k}^n \triangleq -\rho_y(v_{i,j+1,k}^n - 2v_{i,j,k}^n + v_{i,j-1,k}^n) \quad (13)$$

$$A_3v_{i,j,k}^n \triangleq -\rho_z(v_{i,j,k+1}^n - 2v_{i,j,k}^n + v_{i,j,k-1}^n) \quad (14)$$

$$c_0 \triangleq \frac{1}{(\triangle t)^2}/(\frac{1}{(\triangle t)^2} + \frac{a}{2\triangle t}) \quad (15)$$

$$c_1 \triangleq (\frac{1}{(\triangle t)^2} - \frac{a}{2\triangle t})/(\frac{1}{(\triangle t)^2} + \frac{a}{2\triangle t}). \quad (16)$$

The constants of ρ_x, ρ_y, and ρ_z are

$$\rho_p = \frac{b}{(\triangle p)^2}/(\frac{1}{(\triangle t)^2} + \frac{a}{2\triangle t}) \qquad p = x, y, z. \quad (17)$$

After setting $v_{i,j,k}^{n+1(*)} = 2v_{i,j,k}^n - v_{i,j,k}^{n-1}$ which is a prediction of $v_{i,j,k}^{n+1}$ by the extrapolation method, and splitting Equation (10) by utilizing an ADI procedure as [4], we get the following recursion relations

$$
\begin{aligned}
(I + A_1)v_{i,j,k}^{n+1(1)} &= -(A_2 + A_3)v_{i,j,k}^{n+1(*)} \\
&\quad + (2c_0 v_{i,j,k}^n - c_1 v_{i,j,k}^{n-1}), \quad (18) \\
(I + A_2)v_{i,j,k}^{n+1(2)} &= v_{i,j,k}^{n+1(1)} + A_2 v_{i,j,k}^{n+1(*)}, \quad (19) \\
(I + A_3)v_{i,j,k}^{n+1(3)} &= v_{i,j,k}^{n+1(2)} + A_3 v_{i,j,k}^{n+1(*)}, \quad (20)
\end{aligned}
$$

where $v_{i,j,k}^{n+1(1)}, v_{i,j,k}^{n+1(2)}$ are the intermediate solutions and the desired solution is $v_{i,j,k}^{n+1} = v_{i,j,k}^{n+1(3)}$.

Finally, expanding A_1, A_2, and A_3 on the left hand sides of Equations (18)–(20), we get the 3D TLM-ADI algorithm as in Table 1.

The 3D TLM-ADI Algorithm

Input= $v_{i,j,k}^n, v_{i,j,k}^{n-1} \; \forall i, j, k$ **Output**= $v_{i,j,k}^{n+1} \; \forall i, j, k$

Begin

 Sub-Iteration 1:
 $-\rho_x v_{i+1,j,k}^{n+1(1)} + (1 + 2\rho_x)v_{i,j,k}^{n+1(1)} - \rho_x v_{i-1,j,k}^{n+1(1)}; \; \forall i, j, k$
  $= -(A_2 + A_3)v_{i,j,k}^{n+1(*)} + (2c_0 v_{i,j,k}^n - c_1 v_{i,j,k}^{n-1})$

 Sub-Iteration 2:
 $-\rho_y v_{i,j+1,k}^{n+1(2)} + (1 + 2\rho_y)v_{i,j,k}^{n+1(2)} - \rho_y v_{i,j-1,k}^{n+1(2)}$
  $= v_{i,j,k}^{n+1(1)} + A_2 v_{i,j,k}^{n+1(*)}; \qquad\qquad \forall i, j, k$

 Sub-Iteration 3:
 $-\rho_z v_{i,j,k+1}^{n+1(3)} + (1 + 2\rho_z)v_{i,j,k}^{n+1(3)} - \rho_z v_{i,j,k-1}^{n+1(3)}$
  $= v_{i,j,k}^{n+1(2)} + A_3 v_{i,j,k}^{n+1(*)}; \qquad\qquad \forall i, j, k$

End

Table 1. The 3D TLM-ADI algorithm

III.1 UNCONDITIONAL STABILITY

The general way of verifying the stability of a finite-difference kind algorithm is to put a elemental solution into the algorithm, and make sure that the amplitude of the propagation gain is no more than one. By applying the Von Neumann analysis [15], we can analytically prove that our 3D TLM-ADI method is unconditionally stable. Consider the elemental solution of Equation (8),

$$
v_{i,j,k}^n = K^n e^{I(ik_x \triangle x + jk_y \triangle y + kk_z \triangle z)}, \quad (21)
$$

where k_x, k_y, and k_z are the wavenumbers along the $x-$, $y-$, and $z-$ direction, respectively, and K is propagation gain. Putting this elemental solution into the 3D TLM-ADI algorithm, and with some manipulation we get

$$
K = \frac{\Lambda + c_0 \pm \sqrt{\mathcal{D}}}{(1 + R_x)(1 + R_y)(1 + R_z)} \quad (22)
$$

where R_x, R_y, and R_z are

$$
R_p = 4\rho_p \sin^2(k_p \triangle p/2) \qquad p = x, y, z, \quad (23)
$$

and

$$
\begin{aligned}
\mathcal{D} &= \sqrt{(\Lambda + c_0)^2 - (1 + R_x)(1 + R_y)(1 + R_z)(\Lambda + c_1)} \\
\Lambda &= R_x R_y + R_y R_z + R_z R_x + R_x R_y R_z.
\end{aligned}
$$

By Examining the amplitude of K, we are able to prove that the 3D TLM-ADI algorithm is unconditionally stable in the following theorem.

Theorem 1 *The 3D TLM-ADI algorithm is unconditionally stable.*

Proof: To prove that the 3D TLM-ADI method is unconditionally stable, we need to show the amplitude of the gain factor K is less than or equal to 1. Let's consider the following two cases,

- **Case 1:** $\mathcal{D} \geq 0$
  From Equations (15) and (23), we know that $\Lambda + c_0$ is greater or equal to 0. Hence,

$$
\begin{aligned}
|K| &\leq \frac{\Lambda + c_0 + \sqrt{\mathcal{D}}}{(1 + R_x)(1 + R_y)(1 + R_z)} \\
&= \frac{\Lambda + c_0 + \sqrt{\mathcal{D}}}{\Lambda + c_0 + R_x + R_y + R_z + c_0 - c_1}.
\end{aligned}
$$

  After substituting $\mathcal{D}$ into the above equation and simplifying it, we get $|K| \leq 1$.

- **Case 2:** $\mathcal{D} \leq 0$

$$
\begin{aligned}
|K|^2 &= \frac{\Lambda + c_1}{(1 + R_x)(1 + R_y)(1 + R_z)} \\
&= \frac{\Lambda + \frac{\frac{1}{(\triangle t)^2} - \frac{a}{2\triangle t}}{\frac{1}{(\triangle t)^2} + \frac{a}{2\triangle t}}}{\Lambda + 1 + R_x + R_y + R_z} \\
&\leq 1.
\end{aligned}
$$

Therefore, the 3D TLM-ADI method is unconditionally stable from the above derivations. $\diamondsuit$

III.2 LINEAR RUNTIME

There are three sub-iterations need to be performed for each time step. By analyzing the run time of each sub-iteration as shown in Table 1, we are able to prove the computational load of the 3D TLM-ADI algorithm is linear time at each time step in the following theorem.

Theorem 2 *The run time of 3D TLM-ADI algorithm is $O(N)$ at each time step, where $N = N_x \times N_y \times N_z$ is the number of total nodes.*
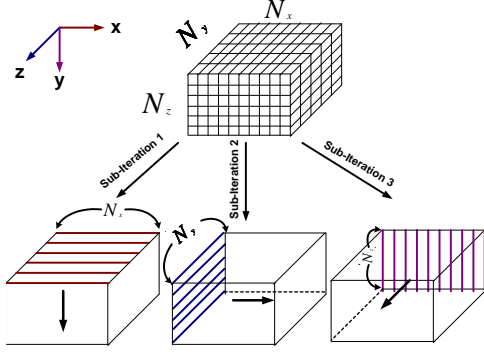
Figure 3. Mesh Points

Proof: Let's consider the Sub-Iteration 1 in Table 1. We can divide the set of these N nodes by $N_y \times N_z$ subsets with each one containing N_x points in the $x-$ direction, as illustrated in Figure 3. Since only three unknown variables need to be solved in the updating equation with each (i, j, k), the coefficient matrix $\mathbf{\Phi}_{j,k}$ associated with updating $v_{\bullet,j,k}'$s is a tridiagonal matrix at each subset. Therefore, the run time of updating $v_{\bullet,j,k}'$s is linear with $O(N_x)$. There are $N_y \times N_z$ subsets in Sub-Iteration 1. Hence, the computational load of the Sub-Iteration 1 is $O(N_x \times N_y \times N_z)$ at each time step.

The run time of Sub-Iteration 2, and 3 is also $O(N)$ by the similar way. Hence, the total run time of the 3D TLM-ADI algorithm is $O(N)$ at each time step. $\diamondsuit$

III.3 NON-UNIFORM GRIDS

Generally, the internodal distance ($\triangle x$, $\triangle y$, and $\triangle z$) may be different for different cells. Hence, we are going to extend the 3D TLM-ADI method to handle this situation, as illustrated in Figure 4. The parameters r, and l are resistance per unit length, and inductance per unit length, respectively. The $C_{i,j,k}$ is the equivalent capacitance, and the $\triangle x_{i\pm1/2,j,k}$, $\triangle y_{i,j\pm1/2,k}$, and $\triangle z_{i,j,k\pm1/2}$ are the internodal distances in the $x-$, $y-$, and $z-$ directions for a cell which the center point is $O_{i,j,k}$, respectively.

We first set up the KCL and KVL equations for each cell, and utilize the same derivation of Equations (8)–(9). The three dimensional telegraph equation becomes

$$\frac{v_{i,j,k}^{n+1} - 2v_{i,j,k}^n + v_{i,j,k}^{n-1}}{(\triangle t)^2} + a\frac{v_{i,j,k}^{n+1} - v_{i,j,k}^{n-1}}{2\triangle t}$$

$$-b_{i,j,k}\left\{ \frac{v_{i-1,j,k}^{n+1} - v_{i,j,k}^{n+1}}{\triangle x_{i-1/2,j,k}} - \frac{v_{i,j,k}^{n+1} - v_{i+1,j,k}^{n+1}}{\triangle x_{i+1/2,j,k}} \right.$$

$$+ \frac{v_{i,j-1,k}^{n+1} - v_{i,j,k}^{n+1}}{\triangle y_{i,j-1/2,k}} - \frac{v_{i,j,k}^{n+1} - v_{i,j+1,k}^{n+1}}{\triangle y_{i,j+1/2,k}}$$

$$\left. + \frac{v_{i,j,k-1}^{n+1} - v_{i,j,k}^{n+1}}{\triangle z_{i,j,k-1/2}} - \frac{v_{i,j,k}^{n+1} - v_{i,j,k+1}^{n+1}}{\triangle z_{i,j,k+1/2}} \right\} = 0 \quad (24)$$

where $a = r/l$, and $b_{i,j,k} = 1/lC_{i,j,k}$.

After utilizing the same procedure of Section III, the recur-

sion relations of the 3D TLM-ADI method for the nonuniform internodal distance case have the same form as Equations (18)–(20) except the definition of the operators, A_m's (see Appendix A).
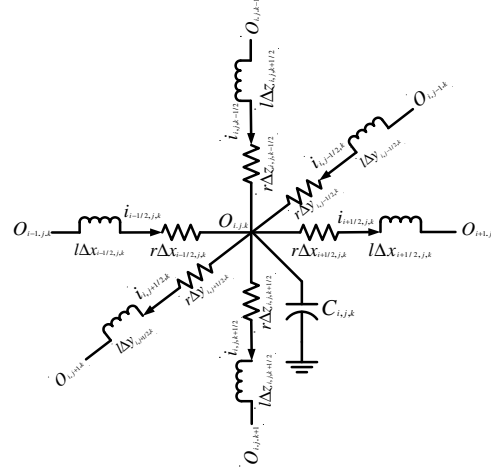

Figure 4. Non-Uniform Internodal Distance Cell

IV EXPERIMENTAL RESULTS

The 3D TLM-ADI algorithm is implemented in C language and performed on a Pentium IV 1.2GHZ machine. The r, l, and c are equal to 0.03 $\Omega/\mu m$, 1.26 $pH/\mu m$, and 0.024 $fF/\mu m$, respectively. The length of each wire segment is between 15 μm and 100 μm, and the resistance of via is 3 Ω. Numerical results are also carried out by using the MNA Solver [1], and the general circuit simulator SPICE.

The comparison of run time and memory usages are shown at Figure 5 with ten time-step period. The power grid model introduced in Section II is used to construct the test sets. The size of the test circuits starts from one thousand three hundred and fifty nodes ($15 \times 15 \times 6$) to one million eight thousand and six hundred nodes ($410 \times 410 \times 6$). Figure 5(a), and (b) show that the 3D TLM-ADI method is not only about 455 times faster than the MNA Solver [1], and over $11,000$ times faster than SPICE even for the grid size is only around $30,000$ nodes ($70 \times 70 \times 6$), but also extremely memory saving. The same tendency that the speed up increases with larger circuit size is
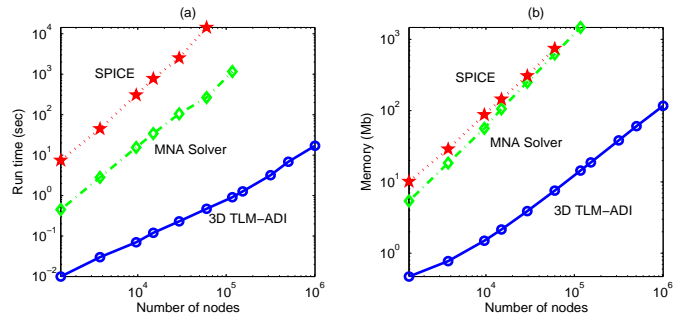

Figure 5. Compare the (a) run time (b) memory usages between the 3D TLM-ADI, PCG and SPICE

also shown in Figure 5(a). Figure 5 also demonstrates that the memory requirement and run time for the 3D TLM-ADI are both linear with the total number of nodes.

To present the accuracy of the 3D TLM-ADI algorithm, we simulate a RLC circuit with nine hundred ($15 \times 15 \times 4$) nodes, and 0.1 ps time step. The Courant stability constraint is 0.31749 ps in this case. Figure 6 shows that the waveform of the 3D TLM-ADI method agrees well as SPICE's at an arbitrary node in the power grids.

The unconditional stability of the 3D TLM-ADI method is demonstrated in Figure 7 with a 75-node RLC circuit. The Courant stability constraint is 1.5874 ps in this case. Figure 7 shows that the time step of the 3D TLM-ADI method is not limited by the above stability constraint but only limited by the accuracy requirement.
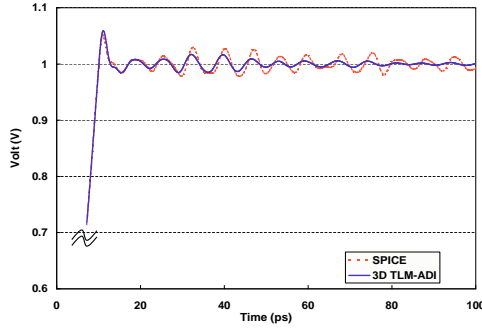

Figure 6. DC transient response comparison between SPICE and the 3D TLM-ADI method

V CONCLUSION

We have developed, and implemented an efficient ADI algorithm for the transient power grids simulation, and proved its unconditional stability and linear run time. The numerical experimental results also show that the 3D TLM-ADI algorithm not only speeds up orders of magnitude over the SPICE but also reduces lots of the memory requirements and the results agree well with the SPICE's.
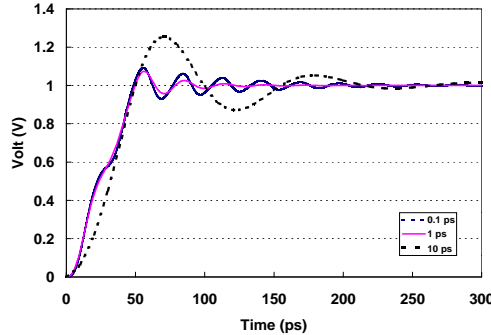
VI ACKNOWLEDGMENTS

Figure 7. DC transient response of the 3D TLM-ADI method with different time steps

References

[1] T.-H. Chen and C. P. Chen. Efficient large-scale power grid analysis based on preconditioned krylov-subspace iterative methods. In *DAC*, pages 559–562, 2001.

[2] C. Christopoulos. *The Transmission-Line Modeling Method TLM*. Oxford University Press, 1995.

[3] A. Dharchoudhury, R. Panda, D. Blaauw, and R. Vaidyanathan. Design and analysis of power distribution networks in PowerPC$^{\text{TM}}$ microprocessors. In *DAC*, pages 738–743, 1998.

[4] J. Douglas and J. E. Gunn. A general formulation of alternating direction implicit methods, part i: Parabolic and hyperbolic problems. *Numer. Math.*, 6:428–453, 1964.

[5] M. K. Gowan, L. L. Biro, and D. B. Jackson. Power considerations in the design of the alpha 21264 microprocessor. In *DAC*, pages 726–731, 1998.

[6] W. K. Gwarek. Analysis of arbitrarily shaped two-dimensional microwave circuits by finite-difference time-domain method. *IEEE Trans. on Microwave Theory and Time-Domain Method*, 36(4):738–744, April 1998.

[7] Y.-M. Jiang and K.-T. Cheng. Analysis of performance impact caused by power supply noise in deep submicron devices. In *DAC*, pages 760–765, 1999.

[8] J.-H. Kim, S. M., and Y. Suh. Modeling of power distribution networks for mixed signal applications. In *IEEE EMC International Symposium*, volume 2, pages 1117–22, 2001.

[9] J. N. Kozhaya, S. R. Nassif, and F. N. Najm. Multigrid-like technique for power grid analysis. In *ICCAD*, pages 480–487, 2001.

[10] Y.-M. Lee and C. P. Che. Power grid transient simulation in linear time based on transmission-line-modeling alternating-direction-implicit method. In *ICCAD*, pages 75–80, 2001.

[11] W. J. Minkowycz, G. E. S. E. M. Sparrow, and R. H. Pletcher. *Handbook of Numerical Heat Transfer*. John Wiely & Sons, Inc., 1988.

[12] L. W. Nagel. Spice2, a computer program to simulate semiconductor circuits. Technical Report ERL-M520, UC-Berkeley, May 1975.

[13] D. W. Peaceman and H. H. Rachford. The numerical solution of parabolic and elliptic differential equations. *J. Soc. Ind. Applicat. Math.*, 3:28–41, 1955.

[14] M. N. O. Sadiku. *Numerical Techniques in Electromagentics*. CRC Press, 1992.

[15] J. C. Strikwerda. *Finite Difference Schemes and Partial Differential Equations*. Wadsworth & Brooks/Cole Advanced Books Software, 1989.

[16] M. Zhao, R. V. Panda, S. S. Sapatnekar, T. Edwards, R. Chaudhry, and D. Blaauw. Hierarchical analysis of power distribution networks. In *DAC*, pages 150–155, 2000.

Appendix A

$$A_1 v_{i,j,k}^n \triangleq -\rho_{i,j,k}\left(\frac{v_{i-1,j,k}^n - v_{i,j,k}^n}{\triangle x_{i-1/2,j,k}} - \frac{v_{i,j,k}^n - v_{i+1,j,k}^n}{\triangle x_{i+1/2,j,k}}\right) \quad (25)$$

$$A_2 v_{i,j,k}^n \triangleq -\rho_{i,j,k}\left(\frac{v_{i,j-1,k}^n - v_{i,j,k}^n}{\triangle y_{i,j-1/2,k}} - \frac{v_{i,j,k}^n - v_{i,j+1,k}^n}{\triangle y_{i,j+1/2,k}}\right) \quad (26)$$

$$A_3 v_{i,j,k}^n \triangleq -\rho_{i,j,k}\left(\frac{v_{i,j,k-1}^n - v_{i,j,k}^n}{\triangle z_{i,j,k-1/2}} - \frac{v_{i,j,k}^n - v_{i,j,k+1}^n}{\triangle z_{i,j,k+1/2}}\right) \quad (27)$$

$$\rho_{i,j,k} = b_{i,j,k}/\left(\frac{1}{(\triangle t)^2} + \frac{a}{2\triangle t}\right) \quad (28)$$